A note on a nonlinear boundary layer model

Geir K. Pedersen

May 20, 2011

1 Introduction

This is a description of method for laminar boundary layer computations. It is assumed that the outer velocity U is extracted from potential flow model or measurements. This is then used as boundary conditions for the boundary layer equations which are discretized by the Crank-Nicholson method for the linear part and a combination of upstream differences and backward time stepping for the nonlinear terms. The grid is generally non-uniform, with finer resolution close to the no-slip boundary, and the technique is validated through comparison with analytic solutions and grid-refinement studies.

2 Boundary layer equations on a beach

We introduce a $(s,z)-$coordinate system with the $s-$axis defined positive upwards along the beach and the $z-$axis orthogonal to the beach. We put $s=0$ at the equilibrium shoreline on the beach. The s- and z-components of the flow outside the boundary layer $U(s,z,t)$ and $W(s,z,t)$, respectively, are supposed known, either from observations or numerical simulations. According to [2], as well as potential flow simulations, the z variation of U is very weak in the swash flow. The flow in a viscous boundary layer, (u,w), is then governed by the following momentum equation

$$\frac{\partial u}{\partial t}+u\frac{\partial u}{\partial s}+w\frac{\partial u}{\partial z}=\left[\frac{\partial U}{\partial t}+U\frac{\partial U}{\partial s}\right]_{z=0}+\nu\frac{\partial^2 u}{\partial z^2}, \tag{1}$$

where the terms within the bracket correspond to the gravity component along the shore and pressure gradient which is assumed equal to that of the outer flow. The continuity equation is

$$\frac{\partial u}{\partial s}+\frac{\partial w}{\partial z}=0 \tag{2}$$

The no-slip boundary conditions is

$$u(s,0,t)=w(s,0,t)=0 \tag{3}$$

and the following matching condition must also be fulfilled

$$\left[u(s,z,t)\right]_{z>>\delta_{bl}}=U(s,0,t) \tag{4}$$

where δ_{bl} is the boundary layer thickness. For the linearized version the boundary value problem given by equations (1) through (4) closed form solutions may be obtained when the outer flows specified as polynomials of time.

3 Numerical computation of boundary layers

3.1 Application of the boundary value model to runup

Outer flow fields are extracted from the inviscid models. The Lagrangian solutions are interpolated onto an equidistant, Eulerian grid along the beach, which extends the whole swash zone, including an extra section on the wet side of off-shore side of the equilibrium shoreline position. An example of the resolution: for solitary waves of amplitude $0.1d$ to $0.3d$ (d is depth of wave tank) incident on 10° beach typically from $M = 50$ to $M = 400$ points have been applied on the beach yielding increments, Δs, in the range $0.22\,\mathrm{cm} \leq \Delta s \leq 1.52\,\mathrm{cm}$. The temporal resolution equals that of the inviscid simulation with time increments down to $\Delta t \approx 0.0004\,\mathrm{sec}$. At a given time only a subset of the Eulerian grid is within the swash zone. During runup new grid points must be included, while points are removed during withdrawal.

In the principle the velocity of the outer flow should have been evaluated at the bottom $z = 0$. However, even though this value may be extracted from the Boussinesq solution [1] we instead use the depth averaged value. The difference is in general very small. The forcing term (within brackets on right hand side) of the momentum equation (1) then becomes $F(s,t) \equiv \frac{\partial U}{\partial t} + U\frac{\partial U}{\partial s}$, where U is the depth averaged velocity from the Boussinesq model, or the bottom velocity from the BIM model.

3.2 Scaling

As the boundary layer method is formulated and implemented in software it may accept input in any consistent scaling, for instance SI units. However, it is convenient to work with dimensionless variables with the depth d as length scale and the shallow water wave celerity $\sqrt{gd}$ as velocity scale. This is the scaling which is used in the Boussinesq and BIM models. The momentum boundary layer equation then reads

$$\frac{\partial u}{\partial t} + u\frac{\partial u}{\partial s} + w\frac{\partial u}{\partial z} = \left[\frac{\partial U}{\partial t} + U\frac{\partial U}{\partial s}\right]_{z=0} + \frac{1}{Re}\frac{\partial^2 u}{\partial z^2}, \tag{5}$$

where $Re = \frac{d\sqrt{gd}}{\nu}$ is a kind of wave-tank Reynolds number. It should be noted that this is not comparable to the standard Reynolds numbers used for stating stability limits for Blasius profiles. In short, the dimensionless kinematic viscosity coefficient is $1/Re$.

3.3 The discretization

A z interval $[0, B]$ is discretized by the grid $\{z_i\}$ such that z_i are given in increasing order with $z_0 = 0$ and $z_N = B$. Generally B corresponds to 2 cm. In the s, z plane we thus have a $M \times N$. Generally the grid is non-uniform in the z direction to allow for a finer resolution close to the boundary $z = 0$. We identify the local grid increments

$$\Delta z_{i+\frac{1}{2}} = z_{i+1} - z_i, \quad \Delta z_i = \frac{1}{2}(z_{i+1} - z_{i-1}).$$

Defining $w_{k,i}^{(n)} \approx w(s_0 + (k-1)\Delta s, z_i, n\Delta t)$, where Δt is the time increment, we discretize the heat equation (1), using the Cranck-Nicholsen method for the linear parts and upwind/backward

representation for the nonlinear parts

$$\frac{u_{k,i}^{(n+1)} - u_{k,i}^{(n)}}{\Delta t} + u_{k,i}^{(n+1)}[\frac{\partial u}{\partial x}]_{k,i}^{(n)} + w_{k,i}^{(n)} \frac{u_{k,i+1}^{(n+1)} - u_{k,i+1}^{(n+1)}}{2\Delta z_i} = \frac{Q_{k,i+\frac{1}{2}}^{(n+\frac{1}{2})} - Q_{k,i-\frac{1}{2}}^{(n+\frac{1}{2})}}{\Delta z_i} + F_k^{(n+\frac{1}{2})}, \quad (6)$$

where

$$Q_{k,i+\frac{1}{2}}^{(n+\frac{1}{2})} = \nu \left(\frac{u_{k,i+1}^{(n+1)} + u_{k,i+1}^{(n)} - u_{k,i}^{(n+1)} - u_{k,i}^{(n)}}{2\Delta z_{i+\frac{1}{2}}} \right),$$

and $[\frac{\partial u}{\partial x}]$ denotes the upwind difference. If an upwind difference involves a value that is not defined, a downwind difference is used instead. The pressure term, F, is consistent with the nonlinear terms on the left hand side of (6). As a consequence the outer flow can be exactly reproduced by the discrete momentum equation. The boundary conditions become

$$u_{k,0}^{(n+1)} = 0, \quad u_{k,N}^{(n+1)} = U_k^{(n+1)}, \quad (7)$$

while w is obtained from the continuity equation according to

$$w_{k,i}^{(n+1)} = \sum_{j=0}^{i-1} \Delta z_{j+\frac{1}{2}} \frac{u_{k+1,j}^{(n+1)} + u_{k+1,j+1}^{(n+1)} - u_{k-1,j}^{(n+1)} - u_{k-1,j+1}^{(n+1)}}{2\Delta s} \quad (8)$$

If k is adjacent to a non-defined s-node (either dry or outside the grid on the seaward side) one sided derivatives are used for u in this expression. When all quantities at time n is known, (6) and (7) yield a set of M, or less, independent tridiagonal equations for the nodal values for u at time $n+1$.

When the shoreline surpasses a new grid point, say m, the row $k = m$ is included in the computation and initial conditions set to $u_{m,i}^{(n)} = U_m^{(n)}$.

The linear version of (6), corresponding to the Crank-Nicholson method, is of second order accuracy and is unconditionally stable. When ν and w are set to zero the discretization corresponds to a second order integration along characteristics. For the combined equation we may no longer claim second order accuracy, but no instability has been encountered. The critical parameter for the accuracy is Δs and the main source of error is linked to the moving shoreline. This is discussed in somewhat more detail below.

3.4 Grid generation

Non-uniform grids, with smoothly varying distribution of nodes, are readily constructed by means of a mapping from a an enumeration coordinate, ζ, to z

$$z = z(\zeta), \quad z(0) = 0, \quad z(N) = B,$$

An approximate local grid increment is then $\Delta z(\zeta) = \frac{\mathrm{d}z}{\mathrm{d}\zeta}$ We desire a finer grid at $z = 0$ than at $z = B$ and define stretch factor, S, as the ratio between the corresponding increments

$$S = \frac{\frac{\mathrm{d}z(n)}{\mathrm{d}\zeta}}{\frac{\mathrm{d}z(0)}{\mathrm{d}\zeta}}.$$

Several distribution functions, f, have been tested, without significant differences in the performance. Two simple nonuniform grids are found as

Quadratic	$z = a\zeta + \frac{1}{2}b\zeta^2$	$a = \frac{2B}{(S+1)N}$	$b = \frac{a(S-1)}{N}$
Exponential	$z = \frac{a}{b}\left(e^{b\zeta} - 1\right)$	$a = \frac{bB}{S-1}$	$b = \frac{\ln S}{N}$

We have mainly employed with $S = 4$.

3.5 Performance

The computations of the boundary layer flow depends on the accuracy of the inviscid simulation in the first place, on the resolution of the extracted outer flow field (Δs) and the vertical resolution in the boundary layer model (N and S). Concerning the modelling of the boundary layer itself there are three main problems that are all linked to the shoreline

1. At the shoreline he physical model of a viscous layer and an outer inviscid flow is not correct. First, in our model the thickness of the boundary layer at a position s grows in proportion to $\sqrt{t - t_0(s)}$, where t_0 is the time when the shoreline reaches s (see equation **??**). In the swash zone the inviscid flow depth will grow in proportion to $t - t_0(s)$. Hence, for small $t - t_0$ the boundary layer will be thicker than the flow depth. Secondly, and more fundamentally, the vicinity of the moving shoreline is governed by some kind of contact point dynamics, where the fluid particle at the shoreline is stuck to the beach, while new fluid presumably is rolled onto the beach during runup. We have not been able to measure any details in the dynamics of the fluid tip and it is beyond modeling at present. Still, only a short distance from the shoreline we do observe a regime with laminar boundary layer motion in the experiments.

2. Also in the linear approximation the initial evolution of the boundary layer is abrupt and thus difficult to reproduce accurately by a numerical technique. However, with the resolutions employed the accuracy in the linear solutions are very good even for quite small times. The next point is more crucial.

3. New grid rows are included in the boundary layer computations in a stepwise manner according to the shoreline motion. At the instant a new row is introduced the velocity is initialized from the outer flow. Consequently there will be a strong along-shore velocity gradient in the boundary layer with a correspondingly large vertical velocity component. This is a plausible mechanism from a physical point of view and it leads to a much faster growth of the boundary layer in the non-linear than in the linear description. However, the mechanism is hard to catch accurately in the numerical model.

In line with the last point the nonlinear solutions are hardest to obtain accurately and the critical parameter is Δs. Therefore we will show some details on the evolution of the boundary value profiles for the most nonlinear case $A/d = 0.295$ in figure 1. At first glance the profiles may look very similar for all times. However, a closer scrutiny reveals a marked deviation for the earliest time displayed, corresponding to a slower boundary layer growth for the coarser resolutions. Later the deviations are diminished. Overall, this indicates that the smallest Δs is adequate.

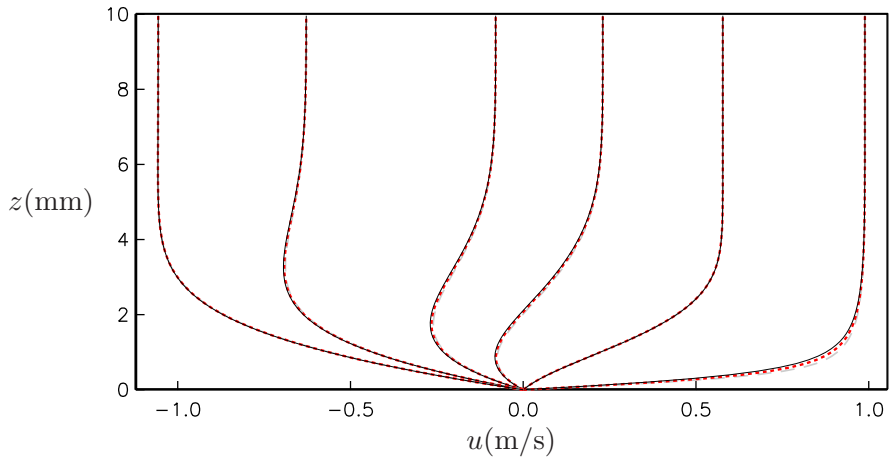

Figure 1: Velocity profiles for $A/d = 0.295$ at $x = 1.05\,\mathrm{m}$. Long dashes, short dashes and solid lines correspond to $\Delta s = 1.52\,\mathrm{cm}$, $\Delta s = 0.76\,\mathrm{cm}$ and $\Delta s = 0.38\,\mathrm{cm}$, respectively. The times are (in seconds) 6.35, 6.55, 6.75, 6.95, 7.35 and 7.70. Since the outer flow is retarded for the range of times displayed, the graphs are ordered from right to left with increasing t.

4 Linear test problems

In this section we neglect the nonlinear terms in (1). The boundary layer equations then become the standard heat equation with a source term F:

$$\frac{\partial w}{\partial t} = \nu \frac{\partial^2 w}{\partial z^2} + F(z,t), \tag{9}$$

where the unknown have been renamed to w. We observe that s does not enter the equation, but may appear only as a parameter.

4.1 Separation of discrete equation

For $F = 0$ the heat equation (9) inherits the simple damped harmonic solutions

$$w = e^{\alpha t} e^{ikz}, \quad \alpha = \nu k^2.$$

For uniform resolution the corresponding solutions for the discrete problem, (6), read

$$w_j^{[n]} = e^{\alpha n \Delta t} e^{ikj\Delta z}, \quad \frac{2}{\Delta t} \tan\left(\frac{\alpha \Delta t}{2}\right) = \nu \frac{4}{\Delta z^2} \sin^2\left(\frac{k\Delta z}{2}\right).$$

This relation always yields a non-negative value for α which implies unconditional stability. Assuming small $\alpha\Delta t$ and $k\Delta z$ we obtain the damping relation

$$\alpha = \nu k^2 \left(1 - \frac{\Delta z^2}{12} k^2 - \frac{\Delta t^2}{12} \nu^2 k^4 + O((k\Delta z)^4, (\alpha \Delta t)^4)\right). \tag{10}$$

Thee is no cancellation of spatial and temporal errors. However, comparable errors due to time and space dicretization occurs when

$$\Delta z^2 \sim \nu^2 k^2 \Delta t^2.$$

Assuming the boundary layer thickness, D, to be of order $1/k$ we find

$$\frac{\Delta t}{\Delta z} \sim \frac{D}{\nu}. \tag{11}$$

This indicate a small time step at the early stages of boundary layer evolution and a much larger step when the boundary layer is well developed. There is absolutely no principal problem employing a variable time step with (6), but this is not yet generally implemented.

4.2 Test problem

The Crank-Nicholson method, as employed in (6) is one of the standard techniques for solution of the heat equation. Still, the implementation must be verified and the performance tested for a relevant boundary value problem. The similarity solution for constant outer velocity is such a problem.

For $U(t) \equiv 1$ and $F \equiv 0$ we have the simple similarity solution

$$w(z) = \frac{2}{\pi} \int_0^{\frac{z}{2\sqrt{\nu t}}} e^{-s^2} ds. \tag{12}$$

As $t \to 0$ the solution becomes discontinuous. Naturally, this feature cannot be captured by the finite difference model. Still, this abrupt onset of the boundary layer is relevant for the swash zone in run-up on beaches and it is crucial that the model rapidly produce a reasonably good solution even though the very first phase of the boundary layer evolution is beyond its capacity.

The criterion (11) now yields

$$\frac{\Delta t}{\Delta z} \sim \sqrt{\frac{t}{\nu}}.$$

Of course, for fixed grid increments and small t the power expansion leading to (10), and thereby to (11), becomes inappropriate. Formally, a relative error measure , E, of (10) become

$$E = \frac{\Delta z^2}{48\nu t} + \frac{\Delta t^2}{192 t^2},$$

where the factors in the denominators are speculative, but they are hardly less appropriate than 1. For a given resolution the above expression may tell at which t we may hope to obtain reasonable numerical results. Still, boundary layer development is an accumulative process and the inadequacy of the numerical procedure in relation to the initial discontinuity in the velocity profile may prevail for quite some time after the local error measure E becomes small.

Preferably, an error analysis should be based on the particular solution (12) instead of simple harmonics. However, even though local discretization errors may readily be estimated it is a challenging task to link this to errors in the solution itself, particularly in view of the singularity at $t = 0$. Hence, we resort to numerical testing, for now.

If the figures 2 and 3 results for a moderately large and a large time are displayed. We immediately observe that the similarity solution is reproduced well.

- For $t = 0.2\,\mathrm{s}$ we observe that convergence appears to more sensitive to Δt than to E.
- For $t = 2.0\,\mathrm{s}$ the given size of Δz for the exponential grid may not be relevant since the smallest Δz is listed in the caption.

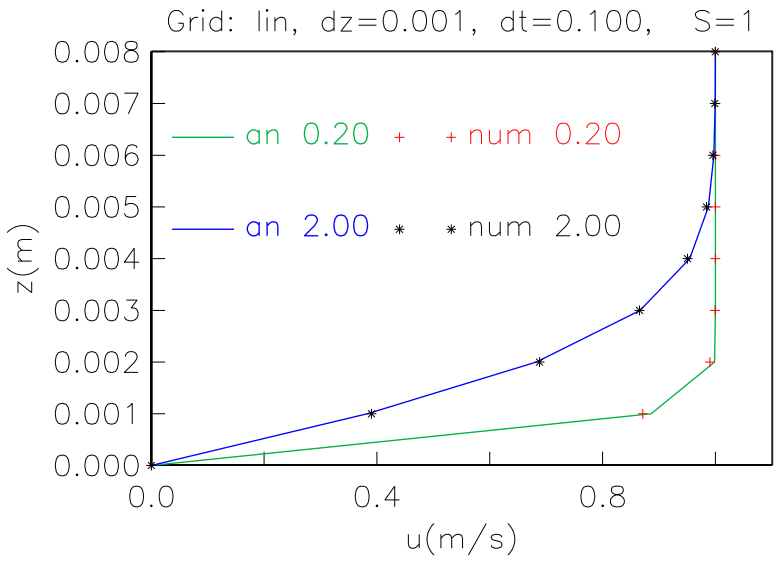

Figure 2: Simulations of similarity profiles for $t = 0.2\,\mathrm{s}$ and $t = 2\,\mathrm{s}$. Times and lengths are given in seconds and meters, respectively. Analytical and numerical results are marked by "an" and "num" respectively.

- For the finer grids there is a striking similarity between the errors for $t = 0.2\,\mathrm{s}$ and $t = 2\,\mathrm{s}$. This indicate that error is dominated by the errors produced in the abrupt start which then are diffused outward.

References

[1] A. Jensen, G. Pedersen, and D. J. Wood. An experimental study of wave run-up at a steep beach. *J. Fluid. Mech.*, 486:161–188, 2003.

[2] G. Sælevik. Ph. d. thesis, Dept. of Mathematics, University of Oslo, 2009.

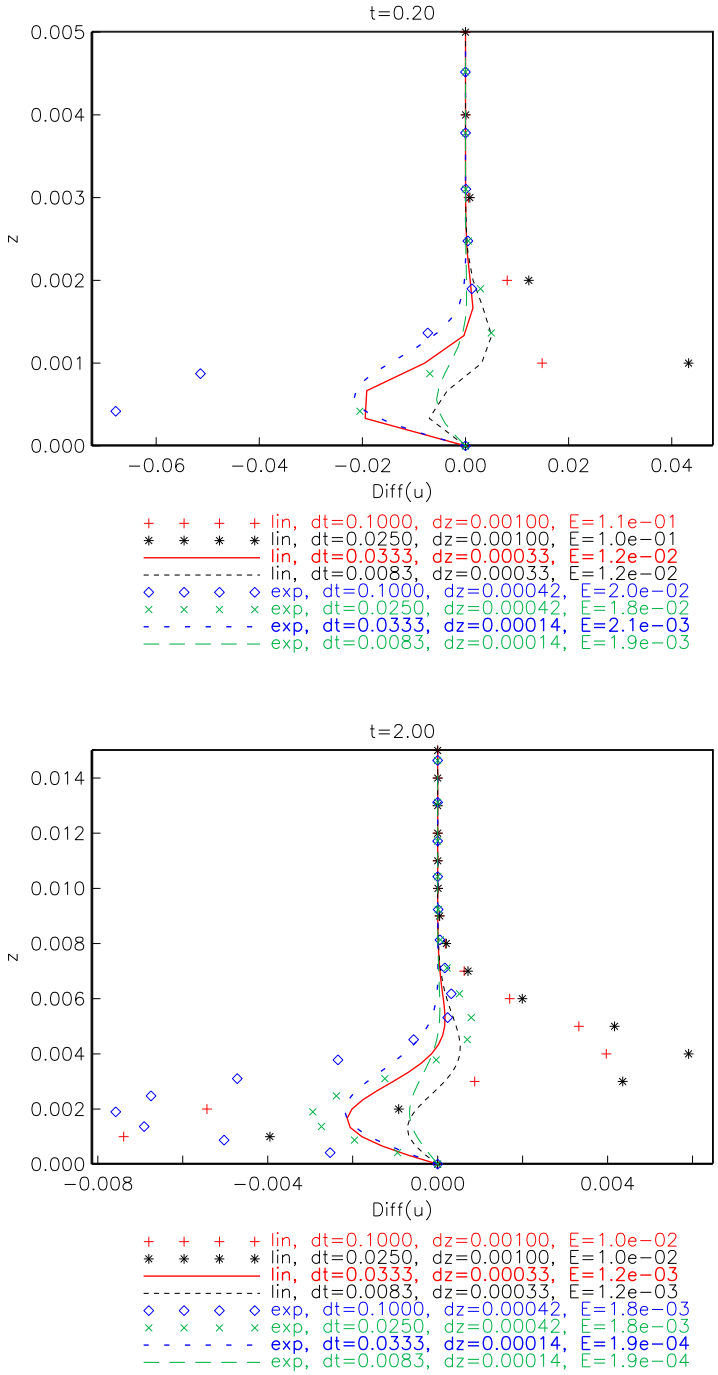

Figure 3: Errors in simulations of similarity profiles. Times and lengths are given in seconds and meters, respectively. For the exponential grids a strech factor $S = 5$ is employed.